Density functional theory calculations of the surface structure of the inverse spinel zinc orthotitanate

2008 J. Phys.: Condens. Matter 20 095001

(http://iopscience.iop.org/0953-8984/20/9/095001)

J. Phys.: Condens. Matter **20** (2008) 095001 (6pp) doi:10.1088/0953-8984/20/9/095001

Density functional theory calculations of the surface structure of the inverse spinel zinc orthotitanate

Rees B Rankin[1], **David S Sholl**[2,3] **and J Karl Johnson**[1,3]

[1] Department of Chemical and Petroleum Engineering, The University of Pittsburgh, Pittsburgh, PA 15261, USA
[2] Department of Chemical Engineering, Carnegie Mellon University, Pittsburgh, PA 15213, USA
[3] The National Energy Technology Laboratory, Pittsburgh, PA 15236, USA

E-mail: karlj@pitt.edu

Received 11 September 2007, in final form 23 December 2007
Published 4 February 2008
Online at stacks.iop.org/JPhysCM/20/095001

Abstract

We present an examination of many different surface terminations of Zn_2TiO_4 (ZTO) obtained by density functional theory calculations. We have examined a total of 41 surface terminations generated from the {001}, {011}, and {111} families of surfaces. Termination of the anisotropic bulk structure of ZTO can produce asymmetric corrugated surfaces that possibly include surface termination artifacts. We have addressed this issue with surface 'smoothing' via atomic transposition of individual atoms across the slab. This procedure reduces the energy penalty associated with large geometric corrugations in the surface layer, particularly in the case of ZTO(111) surfaces. The interface with the lowest energy was found to be a termination of the ZTO(010) surface having a surface formation energy of 1.09 J m^{-2}. A moderately higher energy surface termination was found for the ZTO(110) surface. This ZTO(110) surface has a surface formation energy approximately 0.1 J m^{-2} higher than that of the lowest energy ZTO(010) surface.

S Supplementary data are available from stacks.iop.org/JPhysCM/20/095001

(Some figures in this article are in colour only in the electronic version)

1. Introduction

The development of high efficiency and high throughput contaminant removal processes is a prerequisite for the utilization of coal as a clean energy source in processes such as integrated gasification combined cycle (IGCC). Current technologies in the IGCC offer a multi-stage/material process for the production of H_2 with contaminant removal. The development of a multi-component contaminant removal sorbent material would offer efficiency gains through process intensification. It is well known that metal oxides such as zinc orthotitanate, Zn_2TiO_4 (henceforth 'ZTO'), offer good thermal stability combined with reactive surface chemistry in the application of hot coal gas cleanup of multiple contaminant species such as H_2S, As, Se [1]. It has been shown that ZTO offers repeatable sorbent generation with acceptable performance loss [2–6]. Despite the potential usefulness of this material for multi-contaminant removal, little atomic-level information is available about the surface structure and properties of ZTO. We know of no information on the relative stabilities of the various possible surfaces of clean ZTO. First principles density functional theory (DFT) has been an invaluable tool for providing information on surfaces and surface processes related to heterogeneous catalysis, both in conjunction with experimental data and prior to the availability of detailed experiments [7–11]. Atomic scale DFT calculations can also provide input for development of meso- and macro-scale models, such as kinetic Monte Carlo or continuum-level process control models.

Rankin *et al* [12] have previously identified the low energy bulk ground state structure of ZTO through the combined use of DFT calculations, cluster expansion Monte Carlo

simulations, and EXAFS (extended x-ray absorption fine structure) measurements. That work provided the first atomic scale picture of both the ground state and finite temperature structures of bulk ZTO. In this paper we use DFT calculations to provide quantitative structural and energetic data about ZTO surface structures. We identify low energy surfaces that are likely to be present on ZTO materials used as sorbents. Thus, our work provides a fundamental understanding of the surfaces that should be considered in contaminant adsorption and dissociation. We are not aware of any experimental studies on the atomic scale structure of the ZTO surface.

2. Calculation methods

Our calculations employed plane wave density functional theory via the Vienna *ab initio* simulation package (VASP) [13, 14]. These calculations utilized both ultra-soft pseudopotentials (USPP) [15, 16] and the projector augmented wave (PAW) approach [17, 18]. We have used the PW91 GGA functional [19] in all calculations. In our USPP-GGA (PAW-GGA) calculations, we used a plane wave cutoff energy of 400 (430) eV. The geometries of the structures in our calculations were relaxed via a conjugate gradient algorithm until the forces on all unconstrained atoms were less than 0.03 eV Å^{-1}. Unless we state otherwise, converged geometries and energies of surface structures of ZTO in the results presented in this paper are produced using calculations with k-space sampled using at least a $3 \times 3 \times 1$ Monkhorst–Pack k-point grid. In our surface calculations, we used slabs in which the vacuum spacing is equivalent to, or slightly greater than, the slab thickness. Calculation slabs ranged from approximately 8.5–12 Å in thickness.

3. Results

Based on the crystal structure of bulk ZTO [12, 20] and the available literature of spinel surface structures [21–30], we have restricted our calculations to examine surface terminations generated from the families of low Miller index surfaces: {001}, {011}, and {111}. We have computed the average surface formation energy, E_{surf}, in order to quantify the relative stability of different surfaces, where E_{surf} [31–33] is given by

$$E_{\text{surf}} = \frac{1}{2A}(E_{\text{slab}} - nE_{\text{bulk}}). \quad (1)$$

Here, E_{surf} is the surface formation energy, A is the surface area, E_{slab} is the DFT computed slab energy, E_{bulk} is the DFT computed bulk energy per unit cell, and n is the number of bulk unit cells comprising the surface slab supercell. The factor of $1/2$ comes from averaging over both sides of the slab. An important restriction of this expression is that the net stoichiometry of the slab in the surface calculations must be identical to the bulk material. All calculations described below satisfied this restriction. The bulk anisotropy of ZTO dictates that a strictly stoichiometric slab calculation will typically possess asymmetrically terminated sides. That is, the top surface will be the complement of the bottom surface, but these surfaces will, in general, not be identical. Therefore, E_{surf} is an average quantity that is not necessarily equal to the individual surface energy of either side of the slab. If both sides of the slab have similar corrugation then E_{surf} will be close to these individual surface energies. However, if the two exposed surfaces are highly asymmetric then there is no way to deconvolute the contribution from each surface.

Table 1. Calculated surface energies for a variety of low Miller index surfaces of ZTO terminated at $z = 0$. All values for E_{surf} are reported in J m^{-2}. Surface smoothing was not performed for these systems.

Surface index	E_{surf}
(001)	1.2
(010)	1.4
(100)	1.4
(101)	2.2
(110)	2.1
(011)	2.2
(111)	2.5

In all our surface calculations the innermost 50% (∼4.25–6 Å) of the atoms in the slab were constrained while the remaining atoms were relaxed. At this point we have ignored possible surface reconstruction effects. We have also not considered oxidation of the surface layers because our future work will initially focus on examining adsorption of contaminants from the reducing environments relevant in IGCC processes.

To obtain different ZTO surfaces, we began with the low energy bulk structure previously identified for ZTO [12]. We generated Miller index surfaces by first rotating the bulk supercell to align the z-axis in traditional Cartesian coordinates to the chosen Miller index. From this point, the newly rotated supercell can be truncated at an arbitrary z coordinate to expose the Miller index surface of interest on one side of the supercell. Finally, the opposing side is truncated at the corresponding z coordinate to create a supercell slab having the complementary surface of the desired Miller index. We applied dipole corrections parallel to the surface normal to account for the artificial dipoles induced in the calculation cell due to the asymmetric slabs [34–36].

Cleaving bulk ZTO to a given Miller index surface can yield multiple distinct terminations of each surface because of the internal structure that exists within the material's unit cell [37–40]. Once the bulk structure of ZTO has been rotated to align the chosen Miller index direction with the conventional z axis, a plane of truncation must be defined to complete the construction of the surface. In our initial calculations, we examined a subset of possible surfaces where this plane was taken at $z = 0$ for the slab's top side. In these calculations, the origin defined by the bulk unit cell in earlier work was used [12, 20]. Values from USPP-GGA calculations with $3 \times 3 \times 1$ k-points for E_{surf} are presented in table 1. The choice of a z coordinate for truncation is arbitrary; to fully explore the terminations possible for a particular Miller index surface, the plane of truncation must be systematically varied throughout the values made possible by the periodicity of the material along the surface normal [37–40]. This means that the results in table 1 should be viewed as giving a first

Table 2. The atomic densities for the surfaces presented in table 1 at varying depths into the surface before and after geometric relaxation. For each termination, data are presented for the top and bottom sides of the calculation slab, respectively (above/below). Results before (after) relaxation are shown at cutoff depths into the slab of 1.0 and 1.5 Å in the left (right) columns.

	Before relaxation		After relaxation	
Surface	1.0 Å	1.5 Å	1.0 Å	1.5 Å
(001)	0.082	0.109	0.192	0.128
	0.164	0.128	0.192	0.128
(010)	0.082	0.128	0.192	0.128
	0.164	0.128	0.192	0.128
(100)	0.082	0.128	0.192	0.128
	0.164	0.128	0.192	0.128
(110)	0.116	0.129	0.116	0.103
	0.039	0.077	0.058	0.065
(101)	0.116	0.103	0.106	0.11
	0.029	0.077	0.068	0.084
(011)	0.010	0.058	0.029	0.071
	0.145	0.110	0.145	0.097
(111)	0.142	0.095	0.174	0.179
	0.047	0.053	0.063	0.116

indication of the properties of the ZTO surfaces. It should be noted that the (100), (010), and (001) surfaces of ZTO are not necessarily identical. As might be expected, our calculations indicate that surface terminations with more undercoordinated atoms (relative to bulk coordination) and those that thus feature geometric 'corrugation', are higher in energy than those with fewer undercoordinated atoms. In these initial calculations, the {001} family of surfaces had the lowest values of E_{surf}, while the (111) surface had the highest values.

We extended our initial calculations by systematically varying the plane of truncation for each surface, exposing the various possible surface terminations that can exist on these surfaces. We found that the surface energies for the ZTO{111} surfaces are especially sensitive to the choice of location of the surface plane (see table SI.1 (available at stacks.iop.org/JPhysCM/20/095001) for detailed information). This effect can be on the order of 70% for some of the ZTO(111) surface terminations. In contrast, the more bulk-like surface terminations exposed by the ZTO{100} family of surfaces exhibit variations in E_{surf} of about 20% as the plane of truncation is varied. The ZTO(111) surface terminations feature more undercoordinated surface layer atoms and therefore have larger deviations in E_{surf} as a function of the location of the surface plane.

One metric for describing surface relaxation in our calculations is the atomic density in the region near the surface. Atomic densities measured at 1.0 and 1.5 Å deep into the surface are presented in table 2, both before and after geometric relaxation. The depth into the surface is measured from the center of the highest atom on the surface along the direction of the surface normal. The results in table 2 are for the same surface terminations described in table 1. The bulk density of ZTO is 0.091 atoms Å^{-3}. In the {001} family of surfaces, the atomic relaxation at a depth of 1.5 Å is reasonably symmetric with respect to the two slides of the slab and can approach a bulk-like density of ∼0.1 atom Å^{-3}. Conversely, the Miller index surfaces from the {011} and {111} families we initially sampled relax in a less symmetric way to densities further from the bulk density. In the lowest energy surfaces, relaxation in the outermost oxygen atoms is typically seen to be approximately 0.2–0.4 Å with respect to the surface normal coordinate direction. For titanium and zinc atoms, the corresponding values are typically about 0.0–0.2 Å, and 0.4–0.5 Å, respectively.

Because of the relatively complex bulk structure of ZTO, the choice of an arbitrary truncation point for the various Miller indices of ZTO surfaces can result in significant geometric corrugation and atomic undercoordination of atoms, particularly in the case of the {110} and {111} families of surfaces. We have explored an additional method of producing relaxed stoichiometric ZTO surfaces in order to mitigate this corrugation. We started with surfaces constructed as described previously and then moved individual atoms from one surface to the complementary surface on the other side of the slab. This approach can be used, qualitatively speaking, to smooth the effects of undercoordination on both sides of the slab. This approach was especially important in the case of ZTO(111). For example, the truncation of ZTO(111) with the top surface at $z = 0.125$ (in fractional coordinates) yielded $E_{\text{surf}} = 1.61$ J m^{-2}. Moving one undercoordinated Zn atom from the bottom side of the slab to its corresponding position on the top side lowered E_{surf} to 1.42 J m^{-2}. Moving the remaining undercoordinated Ti atom from the bottom side of the slab to the top raised the value of E_{surf} to 1.82 J m^{-2} due to the formation of completely unfilled octahedral rows on that side of the surface slab. In the case of ZTO(010), taking the termination associated with the lowest value of E_{surf} (at the $z = 0.5$ fractional coordinate termination plane) and transposing the undercoordinated Zn atom from the slab's bottom to the slab's top raises the value of E_{surf} from 1.16 to 1.41 J m^{-2}. This rise in energy is associated with moving the undercoordinated Zn to an even more undercoordinated state.

We used calculations of the kind just outlined to examine a large number of possible surface terminations. In the supplementary information table SI.1 (available at stacks.iop.org/JPhysCM/20/095001), the energies for all the surfaces we studied are listed with respect to the choice of the truncation plane in the unit cell. Surfaces that were examined with multiple termination features via moving individual atoms between the top and bottom of the slab are denoted (a), (b), (c), ... The choice of truncation planes in the unit cell were chosen on the basis of the bulk-like 'layer' distance of 1/8th of the unit cell. We have examined a total of 41 different low Miller index surface terminations. The results of these calculations are presented in condensed form in table 3. In this table we present the single lowest observed surface formation energies for ZTO surfaces derived from each of the low Miller index surfaces. These results are for calculations sampling k-space with a $5 \times 5 \times 1$ mesh.

The lowest energy surface we have identified is a termination of the ZTO(010) surface. This surface is shown in figure 1 (top and bottom view), and figure 2 (side view). It can be seen in these figures that the top side of the surface slab of ZTO(010) is more rich in undercoordinated metal atoms

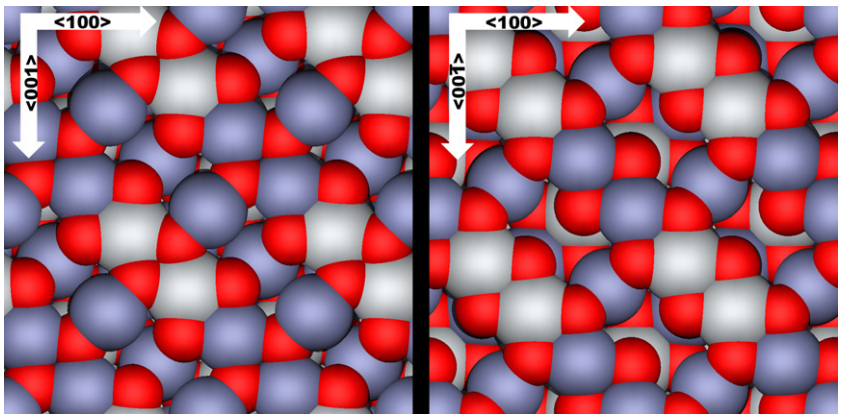

Figure 1. Top (left) and bottom (right) views of the surface termination of ZTO(010) having the lowest energy observed in our calculations. The darkest (red) atoms denote oxygen, the next darkest (blue) denote zinc and the lightest (gray) denote titanium.

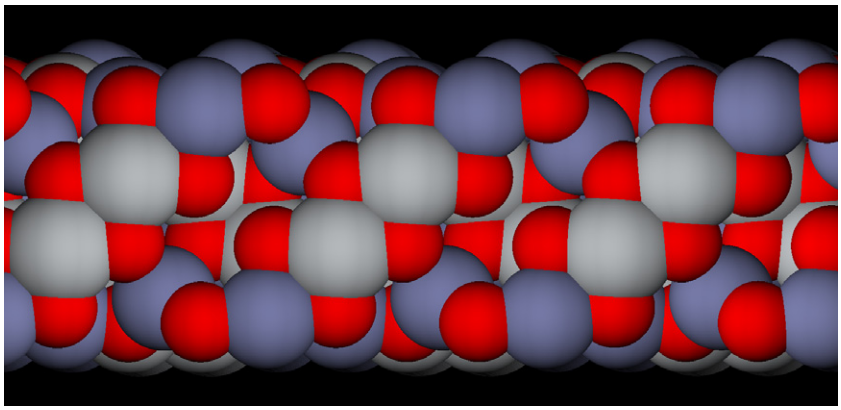

Figure 2. A side view of the same ZTO(010) surface shown in figure 1. The top and bottom sides of the slab show little geometric corrugation. The slab thickness is ∼8.50 Å.

Table 3. The lowest identified E_{surf} values for each of the representative low Miller index surfaces of ZTO. (Additional calculation data is provided in the supplementary information available at stacks.iop.org/JPhysCM/20/095001.) All values for E_{surf} are reported in J m^{-2}. Surface smoothing was performed for these systems.

Surface	E_{surf}
(010)	1.19
(110)	1.28
(100)	1.36
(001)	1.36
(101)	1.40
(111)	1.42

than the bottom side. The Zn atoms bridging the O atoms in octahedral rows in the top side of the slab are undercoordinated relative to the bulk or to the other metal atoms in the surface. The second lowest energy surface termination we identified is a ZTO(110) surface. Top and bottom views of this surface are shown in figure 3. A side view is shown in figure 4. Similar to ZTO(010), it can be seen in figure 3 that ZTO(110) slab also features a side that is slightly more rich in undercoordinated metal atoms.

The low energy surface termination of ZTO(010) exposes the octahedral rows in the bulk that feature Zn–Zn–Ti–Ti–Zn–Zn–Ti–Ti$\cdots$ chains. It is interesting to note that the corresponding type of termination for the ZTO(001) and ZTO(100) surfaces expose octahedral rows with perfectly alternating Zn–Ti–Zn–Ti$\cdots$ chains. The corresponding difference in energy between these surfaces is $+0.17$ J m^{-2}. This is a large energy penalty for a seemingly minor difference in the surface structure. This result is not surprising, however, in view of the previous work we have reported on the bulk structure of ZTO [12]. In that prior work, bulk energy changes typically on the order of 0.5 eV/unit cell were observed for simple switches of cations in the lattice. The reason for this steep energy penalty was found to be twofold: Ti cations having large positive charges, and Ti cations arranging at approximate neighbor distances of 3.02 Å, which is closer than the ideal bulk lattice packing for Ti in an fcc lattice structure.

The ZTO(001) and ZTO(100) surface terminations have Zn–Zn–Ti–Ti–Zn–Zn–Ti–Ti octahedral chain rows running through the slab, but not exposed on the surface. In contrast, the ZTO(010) surface has these Zn–Zn–Ti–Ti–Zn–Zn–Ti–Ti octahedral cation chain oriented parallel to the surface layer, allowing more freedom for relaxing the Ti–Ti distances on the

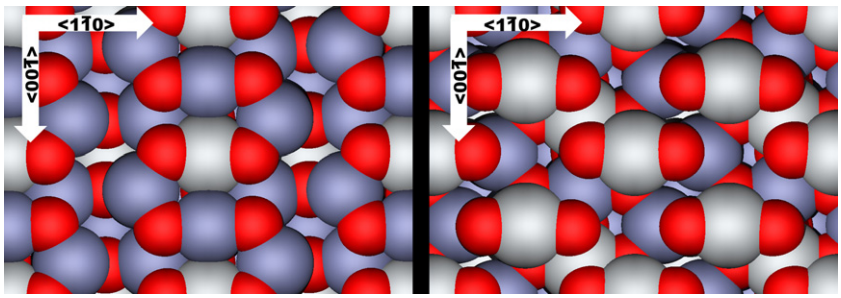

Figure 3. Top (left) and bottom (right) views of the surface termination of ZTO(110) having the second lowest energy observed of all surfaces considered in our calculations. The color scheme is the same as figure 1. These energies are for slabs that are one unit cell thick. Calculations on slabs of two unit cells in thickness gave E_{surf} values of 1.09 and 1.20 J m^{-2} for the (010) and (110) surfaces, respectively.

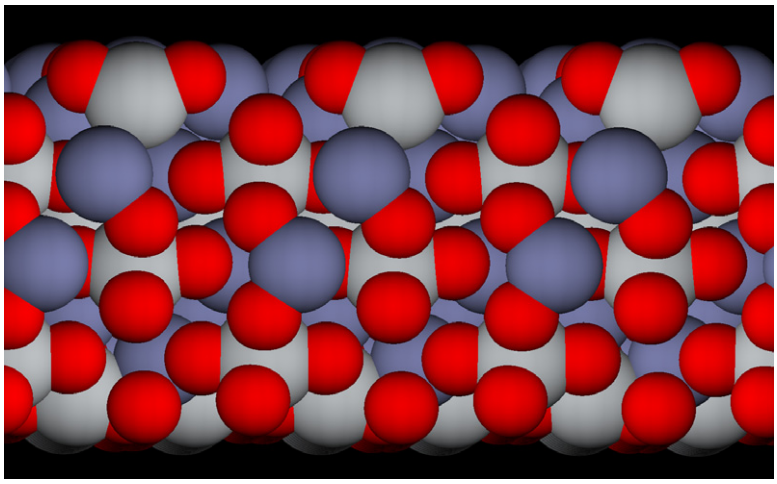

Figure 4. A side view of the same ZTO(110) surface shown in figure 3. The slab thickness is ∼12.05 Å.

exposed surface and hence lowering the total energy. As a result of this, observed Ti–Ti distances in the ZTO(001) surface include values of 2.95, 2.99, 3.05, and 3.11 Å compared to values of 3.08 and 3.32 Å in the ZTO(010) surface.

The slabs used in our surface termination calculations were one unit cell thick. These slabs therefore ranged in thickness from 8.52–12.08 Å, depending on the surface. The thinnest ZTO slabs, such as those of the {001} family of terminations, had relatively thin relaxation layers of ∼2 Å on each side of the slab. In order to quantify the effects that slab thickness and relaxation depth may have on the calculated values of E_{surf} for ZTO surfaces, we have tested these parameters on the two lowest energy ZTO surface terminations in table 3, namely the (010) and (110) surfaces. For the lowest energy ZTO(010) surface, we performed calculations with a slab of twice the original thickness, both with the same relaxation depth and also double the relaxation depth as used in our previous calculation. The value of E_{surf} changed from 1.19 to 1.16 J m^{-2} for the double thickness slab with the same relaxation depth and from 1.19 to 1.09 J m^{-2} for the double thickness slab with twice the relaxation depth. We performed a similar set of calculations for the lowest energy ZTO(110) surface. The value of E_{surf} for this surface changed from 1.28 to 1.22 and 1.20 J m^{-2} for the double thickness slab with the same relaxation depth and with twice the relaxation depth, respectively. The ZTO(110) surface unit cell is inherently thicker than the ZTO(010) surface unit cell (12.08 Å compared with 8.52 Å, respectively). Therefore, the smaller effect on E_{surf} due to a doubling of the slab thickness for the (110) compared with the (010) surface is not surprising. We note that doubling the supercell thickness and the relaxation depth did not qualitatively change our observations.

4. Conclusions

We have surveyed a large number of surface terminations of ZTO in order to gain insight on the surface structure of this material. The following trends were observed in the energy-ordering of the surface terminations we have calculated for ZTO: (1) Surfaces with stoichiometries closest to the bulk-like stoichiometry possessed the lowest surface formation energies. (2) Surface slabs where both sides featured atomic densities closest to the bulk-like density showed the lowest surface formation energies. These results are not unexpected; large surface corrugations and atoms with undercoordinated valence structures would be expected to be higher in energy than the alternative surface terminations due to the greater relaxations required to partially offset the non-bulk-like coordination in bonding. Extreme undercoordination of surface atoms combined with the associated large geometric corrugations induce surface formation energies almost twice as large as those observed in lower energy surfaces. We

note here that with fully relaxed surface energies in the range of 1–2 J m^{-2} for the lowest energy ZTO surfaces, these results are similar to previous theoretical calculations of spinel surfaces [22–24, 26, 27, 29] and inverse spinel surfaces of magnetite [21, 25]. These previous calculations also showed that the {001} family of surfaces had lower energies than the {111} family of surfaces.

The lowest energy termination of ZTO(010) is observed to have a significantly lower value of E_{surf} than the similar lowest energy ZTO(110), ZTO(100), and ZTO(001) surface terminations. Therefore, the surface area associated with the (010) surface should be larger than the latter surfaces on polycrystalline samples of ZTO in thermodynamic equilibrium. It is likely that real ZTO surfaces, such as ZTO(010), have regions that feature both metal rich and oxygen rich domains. This factor is potentially important for understanding why ZTO functions well as a sorbent for IGCC cleanup.

Our results could also be a useful starting point for more detailed studies using the methods of *ab initio* thermodynamics [41–44] to examine the possible surface reconstructions of ZTO surfaces or effects induced on ZTO surfaces by O_2 in an oxidizing environment. Once information from calculations of this type was available, it could potentially be used within the framework of the Wulff construction [45, 46] to predict the equilibrium crystal shape of ZTO crystals in reactive environments.

Acknowledgments

This work was financially supported by NETL via contract DE-AC26-04NT41817, subtask 606.01.04.

References

[1] Shoko E, McLellan B, Dicks A L and da Costa J C D 2006 *Int. J. Coal Geol.* **65** 213
[2] Park N K, Lee D H, Jun J H, Lee J D, Ryu S O, Lee T J, Kim J C and Chang C H 2006 *Fuel* **85** 227
[3] Park N K, Lee D H, Lee J D, Chang W C, Ryu S O and Lee T J 2005 *Fuel* **84** 2158
[4] Park N K, Lee J D, Lee T J, Ryu S O and Chang C H 2005 *Fuel* **84** 2165
[5] Diaz-Somoano M, Lopez-Anton M A and Martinez-Tarazona M R 2004 *Energy Fuels* **18** 1238
[6] Ikenaga N, Ohgaito Y, Matsushima H and Suzuki T 2004 *Fuel* **83** 661
[7] Hafner J, Wolverton C and Ceder G 2006 *MRS Bull.* **31** 659
[8] Hammer B 2006 *Top. Catal.* **37** 3
[9] Hammer B and Nørskov J K 2000 *Adv. Catal.* **45** 71
[10] Greeley J, Nørskov J K and Mavrikakis M 2002 *Annu. Rev. Phys. Chem.* **53** 319
[11] Sholl D S 2006 *Chem. Model.: Appl. Theory* **4** 108
[12] Rankin R B, Campos A, Tian H, Johnson J K, Spivey D, Sholl D S and Siriwardane R 2007 *J. Am. Ceram. Soc.* at press
[13] Kresse G and Hafner J 1993 *Phys. Rev.* B **47** 558
[14] Kresse G and Furthmüller J 1996 *Phys. Rev.* B **54** 11169
[15] Kresse G and Hafner J 1994 *J. Phys.: Condens. Matter* **6** 8245
[16] Vanderbilt D 1990 *Phys. Rev.* B **41** 7892
[17] Blöchl P E 1994 *Phys. Rev.* B **50** 17953
[18] Kresse G and Joubert J 1999 *Phys. Rev.* B **59** 1758
[19] Perdew J P, Chevary J A, Vosko S H, Jackson K A, Pederson M R, Singh D J and Fiolhais C 1992 *Phys. Rev.* B **46** 6671
[20] Bartram S F and Slepetys R A 1961 *J. Am. Ceram. Soc.* **44** 493
[21] Davies M J, Parker S C and Watson G W 1994 *J. Mater. Chem.* **4** 813
[22] Yanina S V and Carter C B 2002 *Surf. Sci.* **513** L402
[23] Pentcheva R, Wendler F, Meyerheim H L, Mortiz W, Jedrecy N and Scheffler M 2005 *Phys. Rev. Lett.* **94** 126101
[24] Hendy S, Walker B, Laycock N and Ryan M 2003 *Phys. Rev.* B **67** 085407
[25] Mariotto G, Murphy S and Shvets I V 2002 *Phys. Rev.* B **66** 245426
[26] Weiss W, Barbieri A, Van Hove M A and Somorjai G A 1993 *Phys. Rev. Lett.* **71** 1848
[27] Anantharaman M R, Reijne S, Jacobs J P, Brongersma H H, Smits R H H and Seshan K 1999 *J. Mater. Sci.* **34** 4279
[28] Shvets I V, Mariotto G, Jordan K, Berdunov N, Kantor R and Murphy S 2004 *Phys. Rev.* B **70** 155406
[29] Schweinfest R, Kostlmeier S, Ernst F, Elsasser C and Wagner T 2001 *Phil. Mag.* A **81** 927
[30] van der Laag N J, Fang C M, de With G, de Wijs G A and Brongersma H H 2005 *J. Am. Ceram. Soc.* **88** 1544
[31] Kokalj A and Causa M 1999 *J. Phys.: Condens. Matter* **11** 7463
[32] Blonski P and Kiejna A 2004 *Vacuum* **74** 179
[33] Da Silva J L F, Barreteau C, Schroeder K and Blugel S 2006 *Phys. Rev.* B **73** 125402
[34] Neugebauer J and Scheffler M 1992 *Phys. Rev.* B **46** 16067
[35] Makov G and Payne M C 1995 *Phys. Rev.* B **51** 4014
[36] Bengtsson L 1999 *Phys. Rev.* B **59** 12302
[37] Asthagiri A and Sholl D S 2004 *J. Mol. Catal.* A **216** 233
[38] Asthagiri A and Sholl D S 2005 *Surf. Sci.* **581** 66
[39] Asthagiri A and Sholl D S 2006 *Phys. Rev.* B **73** 125432
[40] Noguera C 2000 *J. Phys.: Condens. Matter* **12** R367
[41] Reuter K and Scheffler M 2002 *Phys. Rev.* B **65** 035406
[42] Reuter K and Scheffler M 2003 *Phys. Rev. Lett.* **90** 046103
[43] Stampfl C 2005 *Catal. Today* **105** 17
[44] Zhang W, Smith J R and Wang X-G 2004 *Phys. Rev.* B **70** 024103
[45] Honkala K, Hellman A, Remediakis I N, Logadottir A, Carlsson A, Dahl S, Christensen C H and Nørskov J K 2005 *Science* **307** 555
[46] Che J G, Chan C T, Jian W E and Leung T C 1998 *Phys. Rev.* B **57** 1875